Eddy-Current Loss FEA-Based Computation of a Class of CWPMM: a Comparison between Single- and Double-Layer Arrangements

Asma MASMOUDI Ahmed MASMOUDI
Research Unit on Renewable Energies and Electric Vehicles
University of Sfax, Sfax Engineering School, BP W, 3038 Sfax, Tunisia
E-mail: asma_masmoudi@yahoo.fr, a.masmoudi@enis.rnu.tn

Abstract: *The prediction of eddy-current losses is of great importance in AC machines especially in PM brushless ones. This statement is further confirmed when dealing with concentrated winding PM machines (CWPMM). These are characterized by the high harmonic content of their air gap flux densities. Within this topic, the paper is devoted to a 2D finite element analysis (FEA) based assessment of the eddy-current losses in a class of CWPMMs characterized by a 12 slot/10 pole combination. A comparison between the double- and single-layer arrangements is achieved through a cross-section mapping, a local, and an overall analysis of the eddy-current loss density. It has been found that the eddy-current losses of the CWPMM with single-layer arranged armature are almost 8% higher than those of one with double-layer arranged armature, which is confirmed by the respective air gap flux density spectra.*

Keywords: *Concentrated winding permanent magnet machine, eddy-current loss density, finite element analysis, mapping, air gap flux density spectrum.*

1. Introduction

Concentrated winding permanent magnet machines (CWPMMs) are being integrated in many applications due to their high torque density, low torque ripple, high efficiency, wide flux weakening range, and fault-tolerance capability [1]. However, they are characterized by their high contents of space harmonics in the air-gap MMF distribution. These lead to the induction of eddy-current losses in the magnetic circuit made up of iron laminations and permanent magnets (PMs).

For this reason, a prediction of theses losses in preliminary design step is of a great importance to improve the machine efficiency and to avoid the risk of irreversible deterioration of the PM characteristics. The most powerful and reliable way to assess these losses is finite element analysis (FEA).

Several analytical models have been recently proposed for the computation of eddy current losses in both integral slot [2] and fractional slot PM motors [3, 4]. The developed models generally consider several simplifying assumptions which inevitably affect the accuracy of the obtained results.

In [5], *Ishak* et al. developed an analytical model for the prediction of eddy-current losses in the rotor magnets of brushless synchronous machines that have a fractional number of slots per pole. The study covered three types of the armature winding arrangement, which are: (i) double layer slots, (ii) single layer slots, and (iii) single layer slots with the winding wound on wider teeth.

In [6], *Amara* et al. developed an analytical technique for predicting the eddy-current losses in the permanent magnets of the moving armature of a tubular machine. In [7], the same authors studied the iron losses in the stator magnetic circuit of the same machine .

This paper presents an analysis of eddy-current losses of a class of CWPMMs in both laminated core and PMs. The results are computed following a 2D time-stepped FEA. The study includes two 12 slot/10 pole topologies. One of which is equipped with a single-layer arranged armature. The other is equipped with a double-layer arranged armature.

A comparison between the double- and single-layer arrangements is achieved through a cross-section mapping, followed by a local and an overall analysis of the eddy-current density, considering three scenarios:

- no-load operation,
- load operation with demagnetized PMs,
- load operation.

2. FEA Dedicated to Eddy-Current Loss Computation

A time-stepped FEA has been developed in order to predict the core-losses in the PMs of the machines under study. This tool has been selected as far as it is powerful and accurate enabling the computation of the electromagnetic field distributions and many related features.

As it is economically and technically impractical to measure separately the core losses in the different parts of the magnetic circuit, FEA remains one of the most effective tool to predict locally these losses.

In this paper, a transient time-stepped FEA has been considered to predict the eddy-current losses in the PMs and in both stator and rotor laminations, considering the above-cited scenarios.

The numerical developed procedure is based on an edge reordering routine of the transient solver which requires a special air gap discretization.

In order to account for the rotation of the rotor geometry, the air gap FE-mesh is divided in the middle into two regions where the moving elements are linked to the rotor and the stationary ones are attached to the stator. The boundary area is meshed identically into equidistant areas in both separated meshes and have to be meshed similarly in each transient step.

The rotor is run and positioned at each time step such that it does not disturb the integrity of the mesh structure as it moves. In order to fulfill the synchronization condition, the time step Δt is chosen as follows:

$$\Delta t = \frac{p_r}{2\pi f}\ \Delta\theta \qquad (1)$$

where:

- $\Delta\theta$ is the increment of the rotation angle,
- p_r is the rotor pole pair number,
- f is the fundamental frequency.

It is important to choose a sufficient number of time steps as far as the accuracy of the computed features depends on. In the case of the studied machine, given the fact that the pole pair number is equal to unity in the stator and to five in the rotor, no multi-periodicity of the electric and magnetic features with respect to the mechanical ones is expected. As a result, the rotor is moves from 0 to 360-mechanical degrees with a step of 2 degrees.

The used materials are M800-65 for rotor and stator corebacks with a resistivity of $25e^{-8}\Omega m$, and NdFeB for the PMs with a resistivity of $1.3e^{-6}\Omega m$. The armature is fed by three phase sinusoidal currents in the three topologies.

It should be noted that the initial phase current satisfying the condition of production of maximum torque mean value is equal to $7\pi/12$ for the first topology, and $\pi/2$ for the second topology with a frequency of 50Hz yielding a time step of 0.5556ms. Figure 1 shows the flowchart of the developed numerical procedure.

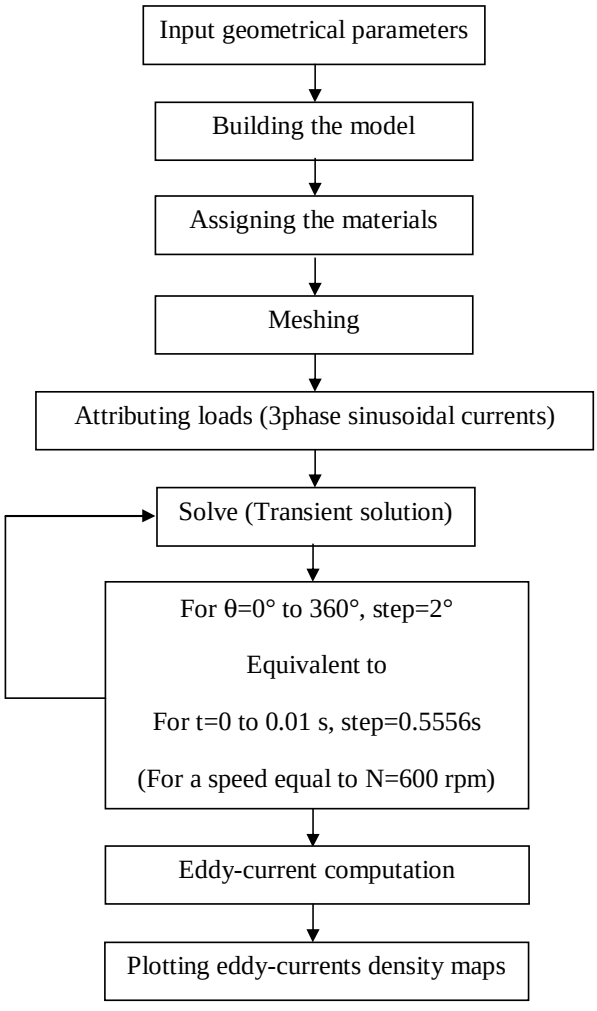

Fig. 1: Flowchart of the developed numerical procedure

3. Case Study

A. Studied Topologies

The study investigates a comparison between two fractional slot PM machines characterized a 12 slot/10 pole combination with double- and single-layer arrangements, respectively. The cross-sections of the machines are shown in figures 2 and 3. The two topologies have the same rotor equipped with ten PMs made up of NdFeB with a radial magnetization.

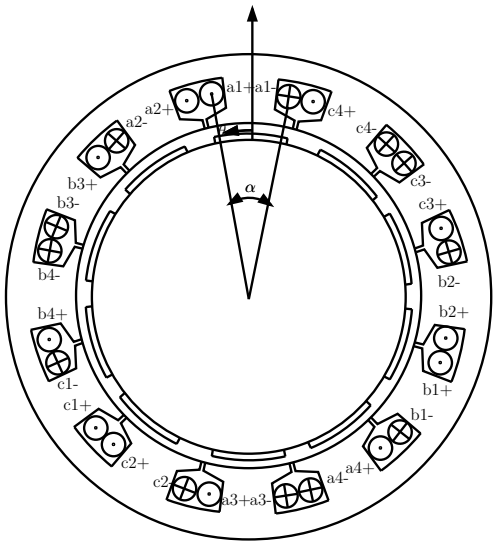

Fig. 2: Double-layer machine layout

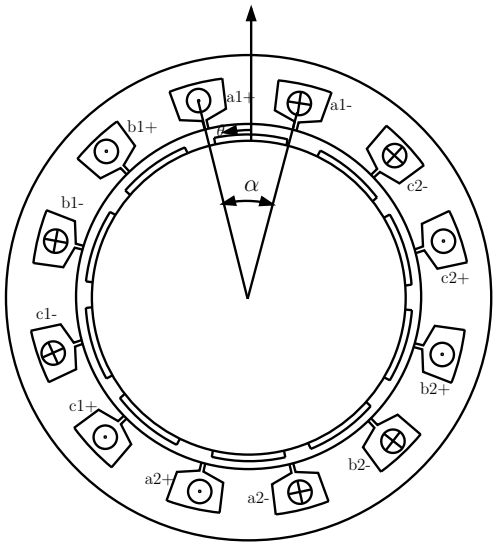

Fig. 3: Single-layer machine layout

The design parameters of the double- and single-layer CWPMMs under study are provided in table 1.

Table 1: Design parameters of the CWPMMs under study

number of phases q	3
number of slots N_s	12
number of poles p_r	10
(coil pitch)/(pole pitch) β	0.125
(magnet width)/(pole pitch) β_{pm}	0.75
rotor outer radius R_{or}	66mm
stator outer radius R_{os}	117mm
air gap δ	0.5mm
permanent magnet height h_{pm}	4mm
permanent magnet resistivity ρ_m	$1.3^{-6}\Omega m$
M800-65 corebacks resistivity ρ_m	$25^{-8}\Omega m$

B. Iron Eddy-Current Mapping

This paragraph is devoted to the presentation of the results yielded by a 2D-FEA related to the analysis of the eddy-current of both machines under study. The analysis concerns the mapping of the eddy-current density in a cross-section, considering the following cases: (i) no-load operation, (ii) load operation with demagnetized PMs, and (iii) load operation, which are illustrated in figures 4, 5, and 6, respectively, where (SLW) indicates single-layer winding and (DLW) indicates double-layer winding.

From these cartographies, one can notice a different variation of the density of eddy-current between the two machines. Referring to the scale associated to these figures, it is to be noted that the red and blue colors indicate high values of the eddy-current densities circulating in positive way and in the negative one, respectively.

Referring to figures 4, 5, and 6, one can notice the following remarks:

- in the case of no-load operation, as far as both machines share the same rotor topology, they have the same eddy-current cartography which is shown in figure 4 at time $t = T$, where T is equal to a mechanical period,
- in the case of $B_r = 0$, one can clearly notice that the eddy-current density has higher values in single-layer machine, as illustrated in figure 5,
- in the case of full-load, a maximum value of the eddy-current density of 6.65 10^5 is reached in the single-layer machine, whereas it does not exceed the 6.46 10^5 in the double-layer one.

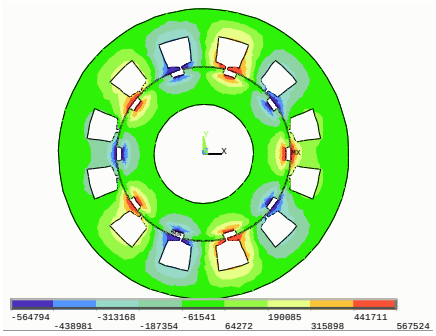

Fig. 4: Eddy-current density at no-load operation

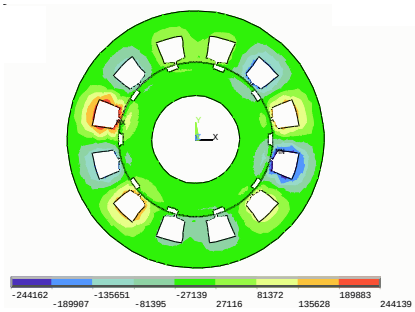

(a)

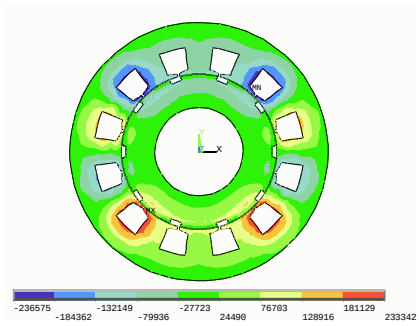

(b)

Fig. 5: Eddy-current density due to armature reaction. Legend: (a) DLW distribution, (b) SLW distribution

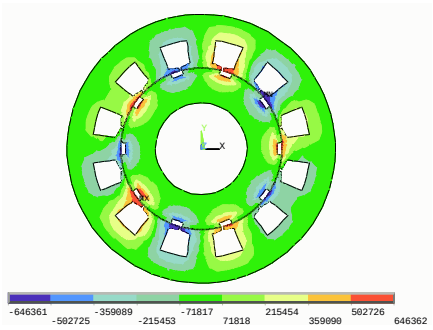

(a)

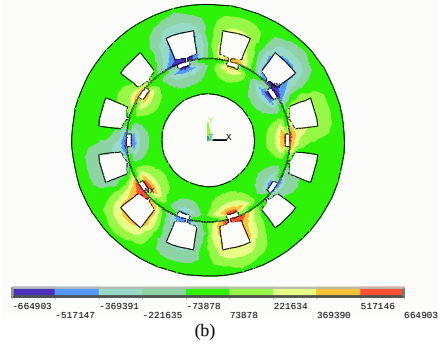

(b)

Fig. 6: Eddy-current density at full-load operation. Legend: (a) DLW distribution, (b) SLW distribution

C. Local Eddy-Current Analysis

In what follows, let us consider the analysis focused upon the eddy-current density versus time in an element located in the middle of a tooth and in one permanent magnet, as illustrated in figure 7.

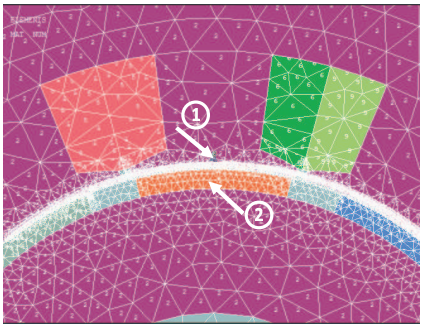

Fig. 7: Zoomed view of a meshed part of the study domain. Legend: ① element in the middle of a tooth, ② a permanent magnet

• Eddy-current Density in the Stator Tooth

Figure 8 shows the variation of the eddy-current density versus time in the element located in the middle of the tooth shown in figure 7 at no load operation. This result concerns both double- and single-layers CWPMMs.

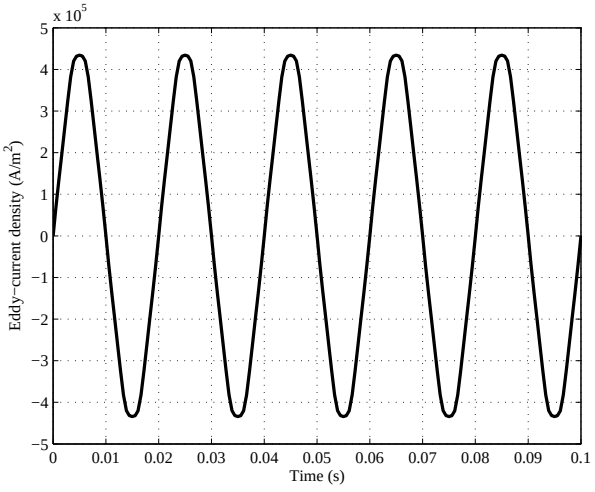

Fig. 8: Eddy-current density in the considered tooth element under no-load operation

Figure 9 illustrates a comparison of the eddy-current density variation with respect to time in both double- (DLW) and in single-layer (SLW) topologies for $B_r = 0$. It is clear that the EC density is higher in the case of SLW. Also, it is to be noted that the two wave forms are shifted which is due to the difference of the current initial phase ψ achieving the condition of maximum torque production, which is equal to $7\pi/12$ in the DLW topology and $\pi/2$ in the SLW one.

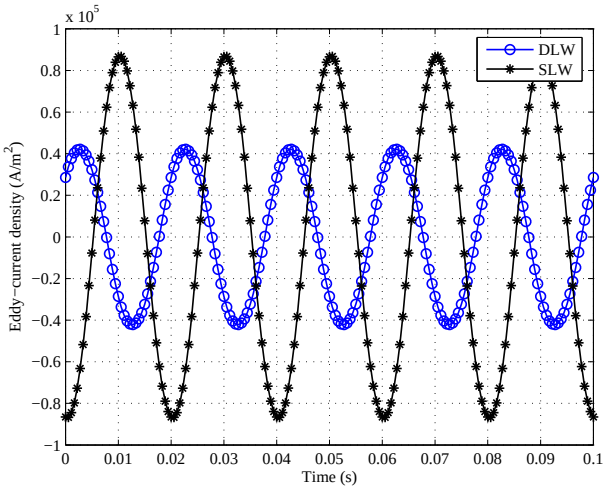

Fig. 9: Eddy-Current density in the considered tooth element for $B_r = 0$

Figure 10 illustrates a comparison of the EC density variation with respect to time in both double- (DLW) and in single-layer (SLW) topologies, at full-load operation.

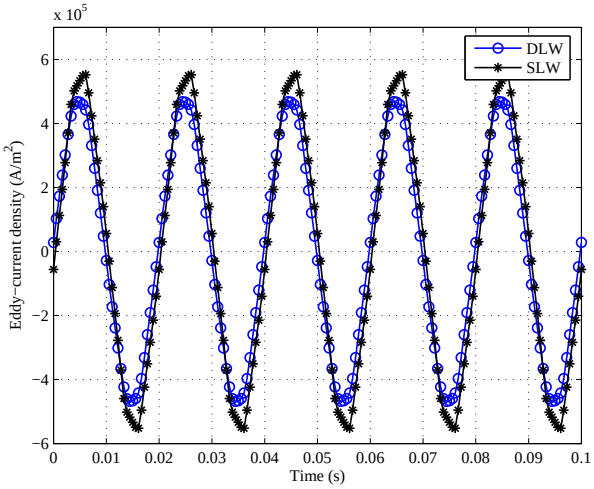

Fig. 10: Eddy-Current density in the considered tooth element under full-load operation

As a conclusion and while comparing figures 8, 9 and 10, one can clearly notice that the EC density at full-load operation is almost the same at no-load one, with the shift between the waveforms of DLW and SLW topologies discarded.

• Eddy-current Density in one PM

Figure 11 illustrates the variation of the EC density in the permanent magnet defined in figure 7 at no-load operation.

Beyond its non-null average value, this density is greatly affected by the slotting effect generated by the variation of the saliency of the stator magnetic circuit.

The slotting effect disturbs the flux density going through the magnet under rotation.

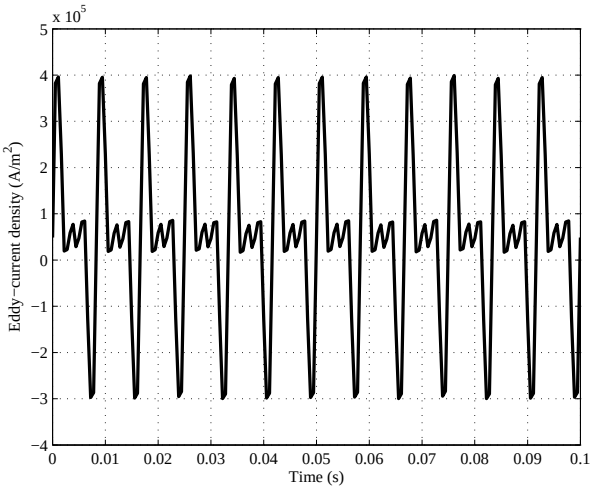

Fig. 11: Eddy-current density in the considered magnet under no-load operation

The above-cited statement is confirmed by the results shown in figure 12 which illustrates the modulation of the flux density in the middle of the permanent magnet by the slotting effect. One can distinguish twelve isolated ripple corresponding to the twelve slots of the stator magnetic circuit.

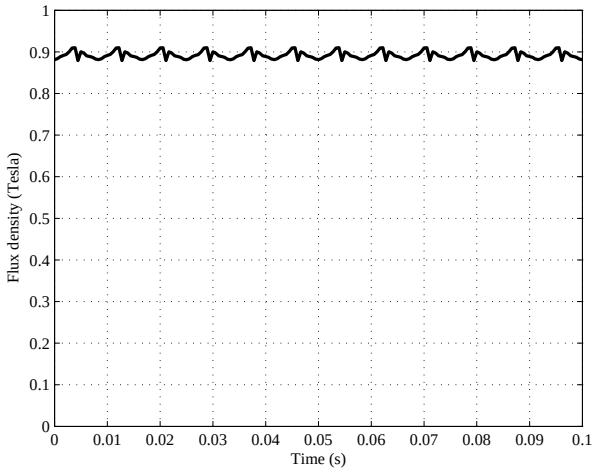

Fig. 12: Flux density in the middle of one magnet under no-load operation

Figure 13 and 16 show the variations with respect to time of the EC density assuming $B_r = 0$ and at full-load operation, respectively. Referring to the results illustrated in figure 11, it is to be noted that the EC density in the magnet is greatly affected by the armature magnetic reaction in the case of ($B_r = 0$) as well as under full-load operation.

The remarkable phenomenon is the ripple affecting the magnet remanence, which is much more significant under full-load operation, as illustrated in figure 15.

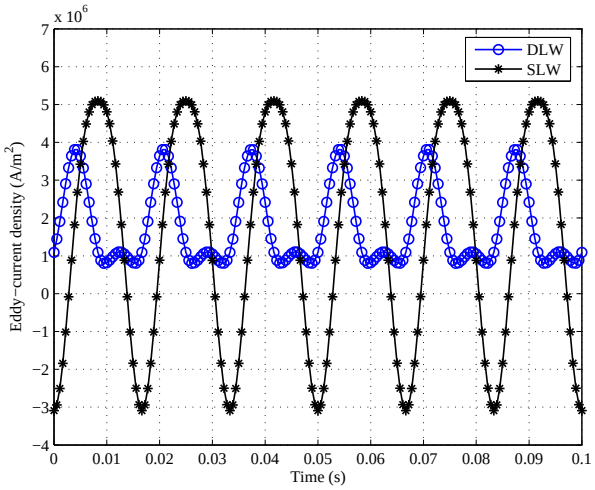

Fig. 13: Eddy-current density in the considered magnet supposed totaly demagnetized

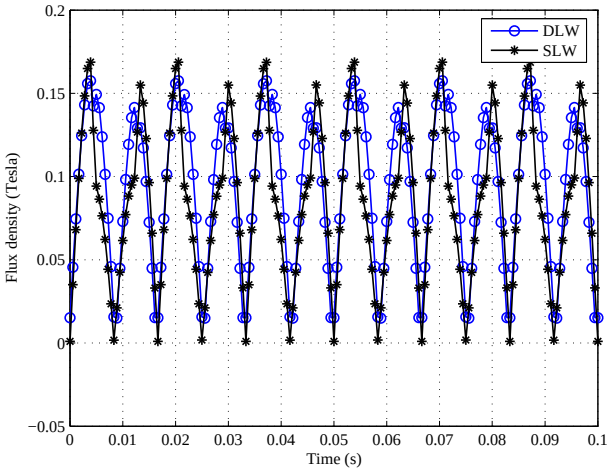

Fig. 14: Flux density in the middle of the considered magnet supposed totaly demagnetized

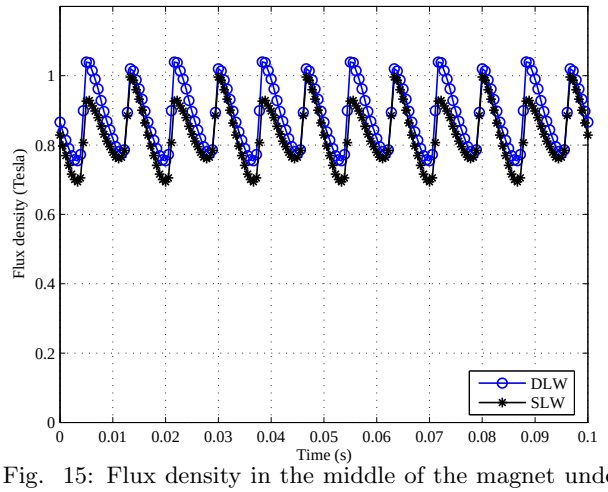

Fig. 15: Flux density in the middle of the magnet under full-load operation

Following the above analysis, one can state that the EC density in PMs are mainly dependent on the armature flux density waveform.

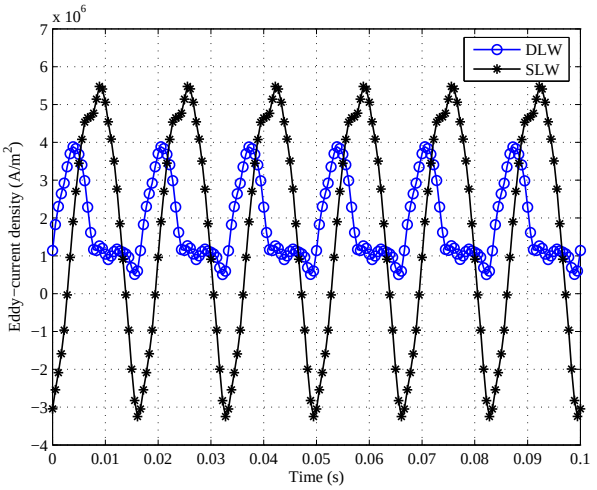

Fig. 16: Eddy-current density in the considered magnet under full-load operation

4. Eddy-Current Loss Overall Analysis

Beyond the local analysis of the eddy-current density (A/m^2), the developed numerical procedure allows the determination of the average value of the eddy-current loss density P_{ec} (W/m) over one period.

The obtained results are provided in tables 2, 3, and 4, in which P_{ec}^{i} and P_{ec}^{pm} refer to the eddy-current loss density in the laminated magnetic circuit including stator and rotor ones, and to the eddy-current loss density in the ten PMs, respectively.

Table 2 presents the EC loss density at no-load operation which is the same for both machines as far as they share the same magnetic circuits.

Table 3 shows the effect of the armature MMF variations causing the induction of eddy current in both machines. As expected, the losses induced in the single-layer CWPMM are higher than those of the double-layer one. This is confirmed by the higher amplitudes of the MMF harmonics, especially the one of rank one, as illustrated in figures 17 and 18, respectively.

Table 4 provides the eddy-current loss densities of both double- and single-layer CWPMMs, at full-load operation. One can remark that these densities are different from the sum of those at no-load and with the magnet demagnetized assumption. This phenomenon is obviously due to the saturation of the magnetic circuit.

Accounting for the results given in tables 2, 3, and 4, one can clearly notice that the major contribution to the eddy-current loss is obtained under no-load operation.

Table 2: EC Loss Density at no-load operation

Topologies	DLW and SLW
P_{ec}^{i}	179W/m
P_{ec}^{pm}	6.16W/m
Total	185.12W/m

Table 3: EC Loss Density with ($B_r = 0$)

Topologies	CW DL	CW SL
P_{ec}^{i}	24.87W/m	40,73W/m
P_{ec}^{pm}	0.27W/m	0.64W/m
Total	25.13W/m	41.37W/m

Table 4: EC Loss Density at full-load operation

Topologies	CW DL	CW SL
P_{ec}^{i}	202W/m	219.7W/m
P_{ec}^{pm}	7.12W/m	6.8W/m
Total	210W/m	226.51W/m

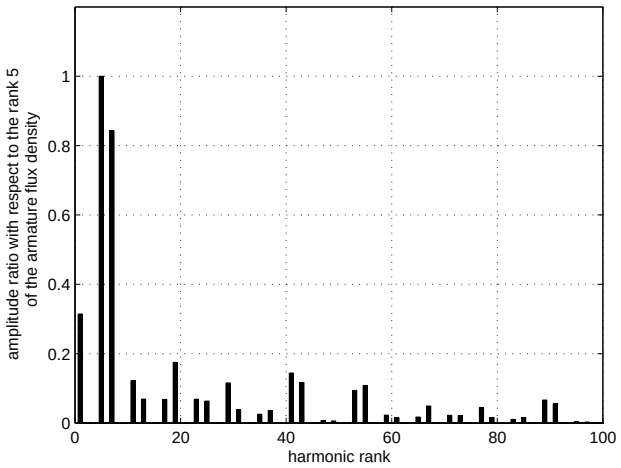

Fig. 17: DL-CWPMM armature MMF harmonic spectrum

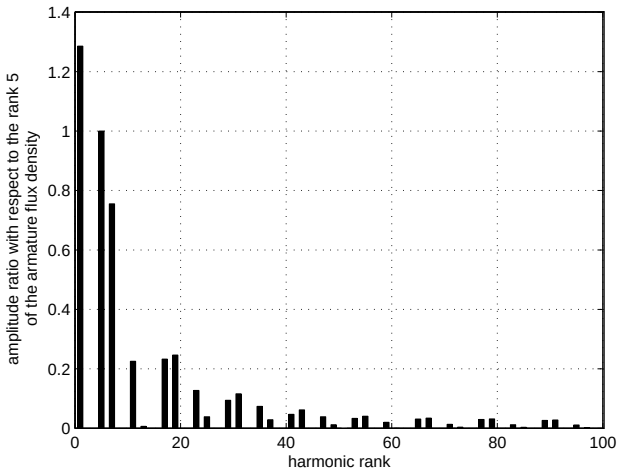

Fig. 18: SL-CWPMM armature MMF harmonic spectrum

5. Conclusion

The paper was devoted to a 2D finite element analysis based assessment of the eddy-current losses in a class of CWPMMs characterized by a 12 slot/10 pole combination. A comparison between the double- and single-layer arrangements has been achieved through a cross-section mapping, a local, and an overall analysis of the eddy-current loss density. No-load, load with PM assumed demagnetized, and full-load operations have been considered to highlight the effect of the flux densities wave forms generated by PMs and armature windings, acting separately and together. It has been found that the eddy-current losses of the CWPMM with single-layer arranged armature are almost 8% higher than those of one with double-layer arranged armature, which is confirmed by the respective air gap MMF harmonic spectra.

References

[1] A. El-Refai, "Fractional Slot Concentrated Windings Synchronous Permanent Magnet Machines: Opportunities and Challenges," *IEEE Transaction on Industrial Electronics*, Vol. 57, No. 1, pp. 107-121, 2010.

[2] C. Mi, G. R. Slemon, and R. Bonert, "Modeling of Iron Losses of Permanent-Magnet Synchronous Motors," *IEEE Transaction on Industry Applications*, Vol. 39, No. 3, pp. 734-742, 2003.

[3] Nicola Bianchi, and Emanuele Fornasiero, "Impact of MMF Space Harmonic on Rotor Losses in Fractional-Slot Permanent-Magnet Machines," *IEEE Transaction on Energy Conversion*, Vol. 24, No. 2,pp.323-328, 2009.

[4] Asma Masmoudi , and Ahmed Masmoudi, "Analytical Prediction of Eddy-Current Losses in Fractional Slot PM Machine," *Journal of Electrical Engineering*, Vol. 10, No. 3, pp. 119-125, 2010.

[5] D. Ishak, Z. Q. Zhu, and D. Howe, "Eddy-Current Loss in the Rotor Magnets of Permanent-Magnet Brushless Machines Having a Fractional Number of Slots Per Pole," *IEEE Transaction on Magnetics*, Vol. 41, No. 9, pp. 2462-2469, 2005.

[6] Y. Amara, J. Wang, and D. Howe, "Analytical Prediction of Eddy-Current Loss in Modular Tubular Permanent-Magnet Machines," *IEEE Transaction on Energy Conversion*, Vol. 20, No. 4, pp. 761-770, 2005.

[7] Y. Amara, J. Wang, and D. Howe, "Stator Iron Loss of Tubular Permanent-Magnet Machines," *IEEE Transaction on Industry Applications*,Vol. 41, No. 4, pp. 989-995, 2005.